41st Aerospace Sciences Meeting and Exhibit
6-9 January 2003, Reno, Nevada

AIAA 2003-0440
Simulation of Micro-Scale Aerodynamics

I.D. Boyd, Q. Sun and M. J. Martin
University of Michigan
Ann Arbor, MI 48109

41st AIAA Aerospace Sciences Meeting
6-9 January 2003 / Reno, NV

SIMULATION OF MICRO-SCALE AERODYNAMICS

Iain D. Boyd†, Quanhua Sun* and Michael J. Martin*
Department of Aerospace Engineering
University of Michigan, Ann Arbor, MI, 48109

Abstract

Despite active development of micro-scale flow technologies for a wide range of applications, very little work has been performed on external aerodynamics at this scale. The present article summarizes our computational and experimental work in this area. The numerical work focuses on development of particle-based algorithms for simulation of the rarefied, nonequilibrium phenomena that occur at the micro-scale. The Information Preservation method is proposed as an effective technique for these flows and is combined with a traditional Navier-Stokes solver in a hybrid continuum-particle algorithm. The experimental work is aimed at measuring data for assessment of the numerical methods. The design of a micro-scale wind-tunnel with low turbulence is presented together with micro-fabrication of a flat plate with integrated force sensors.

1. Introduction

Gas flow around micro-scale structures forms an integral part of many applications of MEMS including micro-turbines, chemical sensors, micro-propulsion for spacecraft, flow control devices, and gaseous chromatographs. Experimental study of micro-scale gas flows is made inherently difficult by the small physical dimensions and has been mainly limited to flows in simple micro-channels and nozzles.[1,2] While there have been a number of recent numerical studies of gas flows in micro-channels,[3,4,5] there has been almost no investigation of gas flows over external bodies at the micro-scale.

Gas dynamics can be classified into continuum, slip, transition, and free-molecular flow regimes. The basic parameter defining these regimes is the ratio of the molecular mean free path (λ, which at standard pressure and temperature for air is about 0.06 micron) to the smallest significant physical dimension characterizing the flow (L, which can be around 1 micron or smaller for MEMS structures), namely the Knudsen number (Kn=λ/L). For such flows, the Knudsen number may be larger than 0.01, which places the flow in the slip (0.01<Kn<0.1) or the transition (0.1<Kn<10) regimes. In these flows, the air in contact with the body surface may have a non-zero tangential velocity relative to the surface (slip), and collisions between molecules and collisions of the molecules with the wall have the same order of probability. These rarefied phenomena must be included in any computer model designed to simulate these flow conditions.

Unfortunately, traditional computational fluid dynamics (CFD) techniques are only valid for the continuum regime (Kn<0.01), and are acceptable for the slip regime if a slip wall condition is adopted instead of non-slip boundary condition. Kinetic-based numerical schemes, such as the direct simulation Monte Carlo (DSMC) method,[6] are more physically appropriate for rarefied gas flows in micro-scale environments. However, the disadvantages of the DSMC method are obvious for micro-flows.[7] It is very difficult for DSMC to isolate the useful signal from the "noise" in low speed flows (micro-flows are usually low subsonic flows). The macroscopic flow velocity is sampled from the velocity of simulated microscopic particles ($V = V_i / N$) and the statistical scatter ($\sigma' = \sigma/\sqrt{N}$) is based on the sampling size. Here, V is the macroscopic flow velocity, V_i is the velocity of an individual particle, N is the sample size for the cell, σ is the physical statistical scatter ($\sigma = \sqrt{2RT}$, R is the specific gas constant, T is the temperature, and σ is about 400m/s for air at standard temperature) and σ' is the final numerical statistical scatter. If we suppose the sample processes in DSMC are totally independent from step to step, then a sample size of 1.6×10^5 is needed to control the statistical scatter within 1m/s, and a sample size of 1.6×10^7 for the scatter to be within 0.1m/s! Hence, few practical micro-flows can be simulated due to the limit of CPU time.[3]

This paper summarizes efforts to develop new computer methods for simulation of micro-scale aerodynamics that have been performed in the last four years in an AFOSR MURI project. The work involves both development and verification of new computer algorithms in addition to the design and construction of a unique experimental testing facility.

2. Numerical Methods

As discussed above, the DSMC technique is unsuitable for low-speed micro-scale gas flows because of problems with excessive statistical fluctuations. An alternative approach is the information preservation (IP) method,[8] which is very effective in reducing the statistical scatter in the DSMC method for low-speed, constant density flow systems. The IP method preserves macroscopic information as well as microscopic information in

† Professor, Associate Fellow AIAA
* Graduate Student Research Assistant, Student Member AIAA

simulated particles as the particles move and interact with each other and the domain boundaries. Within the MURI project, we have implemented several versions of the IP method and applied them to both internal and external flows.[5,9,10,11] Another important type of algorithm for micro-scale gas flows is a hybrid methodology employing continuum (CFD) and kinetic (DSMC, IP) methods in different regions of a flow field dependent on local flow characteristics. A first version of such a CFD-DSMC/IP code has been formulated recently[12] and will be described here briefly.

2.1 Information Preservation Method

It is generally assumed that each particle simulated in the DSMC method represents an enormous number (10^8-10^{25}) of real molecules, and these particles possess random thermal properties according to certain distributions (they are Maxwellian distributions for equilibrium gas flows). Hence, each particle has the microscopic information (molecular position, velocity, internal energy, etc) and the collective information of the represented molecules (velocity, temperature, etc). The information preservation method aims to preserve and update the collective information of the real molecules, intending to reduce the statistical scatter inherent in particle methods. In the paper by Fan and Shen[13], information velocity was preserved and updated by collisions between particles, collisions of particles with the wall and the external force field (the pressure field when gravity is neglected). In our first implementation of the IP method, see Cai et al.,[5] the number density information and velocity information for computational cells were additionally preserved when the IP method was extended to 2D isothermal problems. A similar implementation was used by Fan et al.[9] to rarefied flow over a NACA-0012 airfoil. In a later implementation (Sun and Boyd[10]), number density information, velocity information and temperature information for both particles and computational cells are preserved. The information is updated by collisions between particles, collisions of particles with walls, and the inviscid fluid mechanics equations in the Lagrangian description.

An implementation of the IP method can be summarized as follows (see also Fig. 1):

(1) All the simulated particles and computational cells are assigned the necessary information after the computational domain is set up. Molecular velocity, location, and internal energy are assigned to each particle as in the DSMC method. The number density information, velocity information and temperature information are assigned to both particles and computational cells using the initial flow condition.

(2) The particles are moved using the molecular velocity with the same algorithms and models as the DSMC method.

(3) In a time step Δt, the preserved information may be changed due to the following causes:

- If there are collisions between particles, a simple scheme satisfying general conservation laws is employed to distribute the post-collision information for two collided particles.

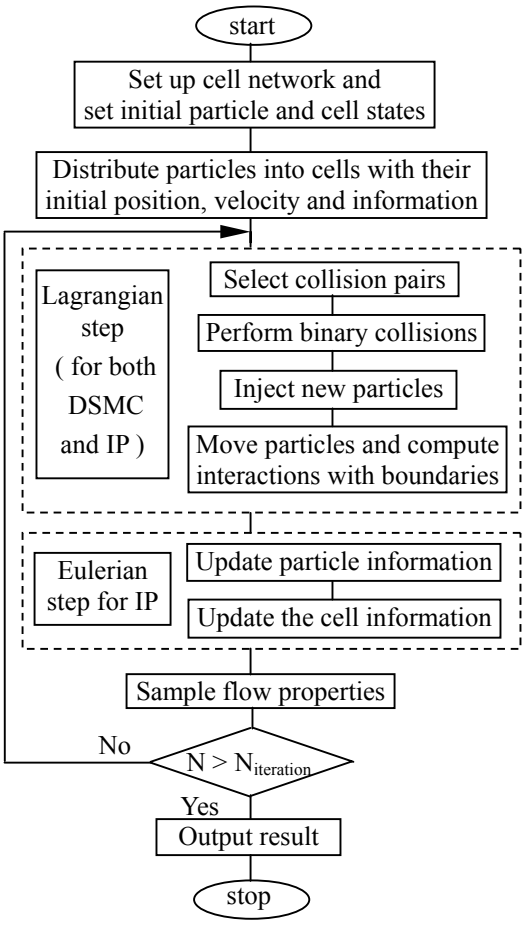

Figure 1. DSMC-IP flowchart

- If there are collisions of particles with a wall, the preserved information of collided particles are set in accordance with the collective behavior of a large number of real molecules. Namely, the information of the particles is set as the wall condition if it is a diffuse reflection while the information velocity component perpendicular to the wall is reversed if it is a specular reflection.
- If particles reflect from a symmetric boundary, the information velocity component perpendicular to the symmetric boundary is reversed.
- If there are new particles entering into the computational domain, their information is set using the boundary condition.
- The preserved information of all particles is updated following the inviscid fluid mechanics equations in the Lagrangian description.

(4) The preserved information of computational cells is calculated from the particles.

(5) Macroscopic quantities are computed based on the preserved information. Field data quantities are accumulated at each sampling step by adding the preserved information of the cell. For surface quantities, free molecular theory is employed based on the pre- and post-collision information of particles collided with the wall since there is no collision between

particles during this process. Like field quantities, surface quantities are sampled by adding the information of collisions between particles and the wall for every incident particle. The final sampled surface quantities are obtained as the accumulated surface quantities divided by the total number of incident particles.

(6) For steady flows, steps 2-4 are repeated until the flow reaches a steady state. Then steps 2-5 are repeated to sample and obtain the macroscopic quantities of the flow.

The above implementation of the IP method can greatly reduce the statistical scatter for low subsonic flows. In DSMC, the statistical scatter comes directly from the thermal movement of particles. In IP, the thermal movement of particles causes statistical scatter only at the information level. Hence the statistical scatter of the information cannot be larger than the variation of the information in the whole flow field. Therefore, the IP method can greatly reduce the statistical scatter and hence the computational cost for low speed flows. The simulation of many practical micro-scale gas flows becomes possible. Another advantage of the IP method is that the preserved information of computational cells has small statistical scatter, and this can help apply effective boundary conditions for the DSMC method for low-speed flows.

2.2 Illustrative IP Results

The IP method has been assessed and verified through its application to a number of different test problems.[5,9,10,11] Figure 2 shows a series of Couette flow velocity profiles obtained over a range of Knudsen number.[10] The excellent agreement between full DSMC results and the IP solutions indicates that the IP method is capable of simulating a wide range of nonequilibrium flow conditions. Figure 3 shows results for a Rayleigh flow problem.[10] This study indicates excellent agreement between full DSMC results and the IP solution for an unsteady problem.

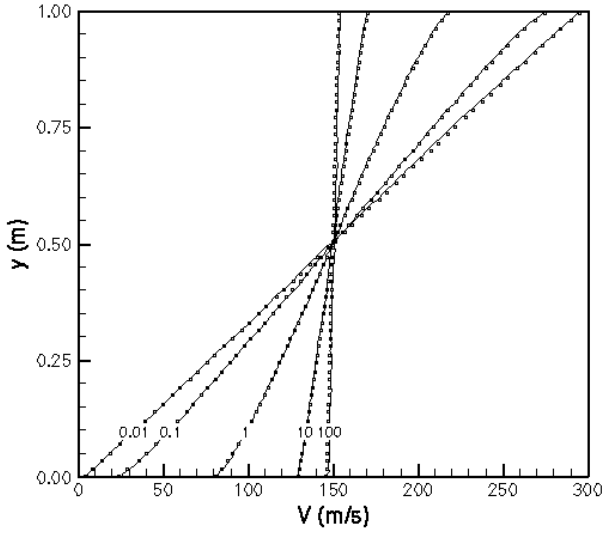

Fig. 2. Velocity profiles for Couette flow (Kn=0.01, 0.1, 1, 10, 100 as labeled in the plot: IP=circle; DSMC=line) from Ref. 10.

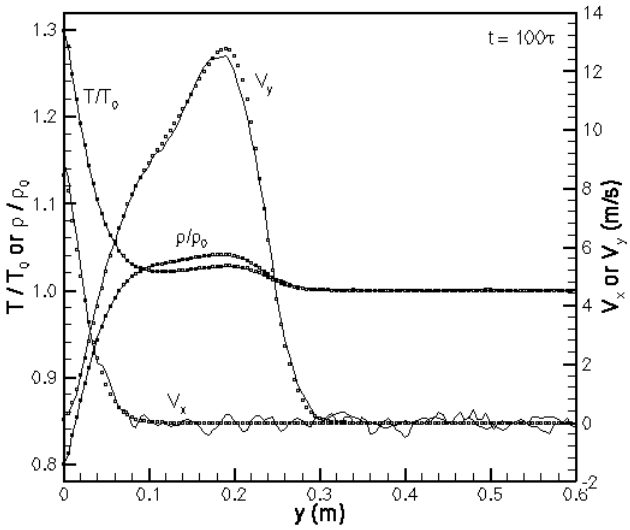

Fig. 3. Profiles for Rayleigh flow at t=100τo (IP=circle; DSMC=line) from Ref. 10.

In terms of external aerodynamics, the problem of rarefied flow past a two-dimensional flat plate aligned with the free stream is one of fundamental interest since it generates a wide range of basic flow phenomena. As the Reynolds number, Re, decreases at a fixed Mach number, M, the nature of the flow changes from continuum to free molecular. Schaaf and Sherman[14] investigated flows over a flat plate experimentally and theoretically in the range of 34<Re<2020 for 2.5<M<3.8 and 3<Re<500 for M of about 0.2 and 0.6. Other theories[15,16,17] are also available for flows from the slip regime to the free-molecular regime. However, theories for flows in the slip and transition regions can only predict flows qualitatively due to the approximations made. The IP method, on the other hand, can simulate the flows at different Reynolds number.

Consider airflow past a flat plat with a finite length of 20 microns. The free stream velocity is about 69 m/s and the Mach number of the free stream is 0.2 with a temperature of

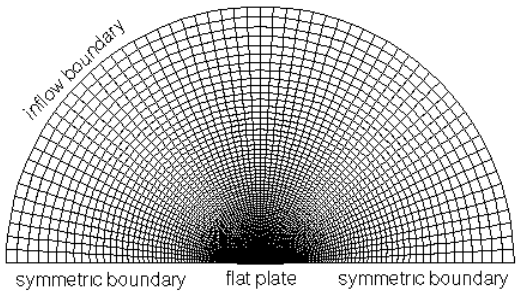

Fig. 4. Computational grid for flow over a flat plate with zero thickness.

295K. The free stream density is determined from the Reynolds number based on the length of the plate. Figure 4 shows the computational domain used in the simulation. The whole domain is divided into 4,800 non-uniform structured cells that are clustered to the plate. On average, 50 particles are located in each cell. When the Reynolds number is larger than 10, a subcell technique is employed with more simulated particles in each cell. For each case, the time step is smaller than the mean collision time of molecules. The given results are only sampled after the skin friction reaches a constant value.

Figure 5 shows the drag coefficient for both sides of the plate at low Reynolds numbers from several techniques. The IP results approach the free molecular theory[18] when the Reynolds number becomes small (Re<0.2) and are close to the numerical solutions of the full Navier-Stokes equations of incompressible flows (Dennis and Dunwoody[16]) when the Reynolds number is greater than 10. The experimental data from Schaaf and Sherman[14] shown in Figure 3 were measured at a Mach number around 0.2 except that the case for the Reynolds number of 3.15 was measured with a Mach number of 0.167. Good agreement is obtained between the experimental data and the IP results except for Reynolds number of 3.15. The difference here probably occurs due to the slightly different Mach number at this condition. The incompressible experimental data of Janour[19] is also plotted in Fig. 5. It seems when the Reynolds number is larger than 10, the difference between the results from the compressible and incompressible flow is very small. Obviously, the Blasius solution of the boundary layer theory[20] is not valid for low Reynolds number flows.

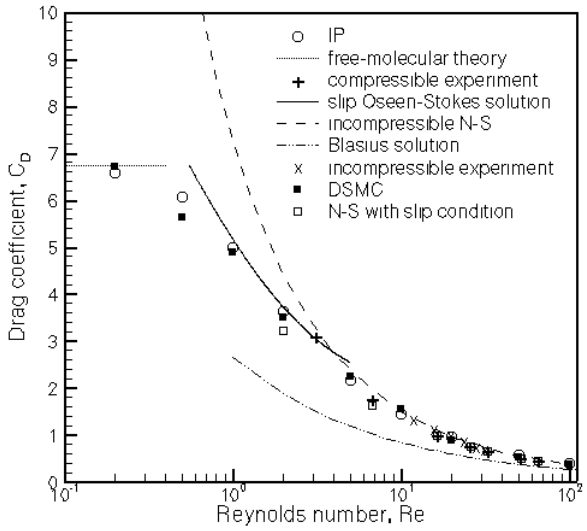

Fig. 5. Drag coefficient of a finite plate at low Reynolds numbers

Having partially verified the IP method for flow over a plate of zero thickness, the same code is applied to investigate the aerodynamics of flow around a plate of finite thickness inclined at an angle of attack. The flow conditions are chosen to correspond to experimental investigations that are being planned (these are described later in this paper). The measurements of Sunada et al.[21] showed that a 5% flat plate had a much larger lift coefficient than NACA airfoils at Re=4,000 for incompressible flows. However, flows over micro-scale structures are usually at much lower Reynolds number.

The 5% flat plate is placed at various angles of attack in an otherwise uniform stream of a gas. The free stream condition is listed in Table 1, and the chord length of the plate is 20 microns. For these calculations, the computational domain extends 5 chord lengths from the airfoil. A total of 11,200 cells is used and about 50 particles are located in each cell. The total sampling size is about 5,000,000 particles per cell after 300,000 iterations are executed with a time step of 2×10^{-11} s. Figure 6 shows the contours of pressure ratio (p/p_∞) close to the flat plate for an angle of attack of 10 deg..

Table 1. Free stream conditions for inclined flat plate flows

Ma_∞	Re_∞	ρ_∞ (kg/m^3)	T_∞ (K)	U_∞ (m/s)
0.087	4.0	0.1176	295	30.0

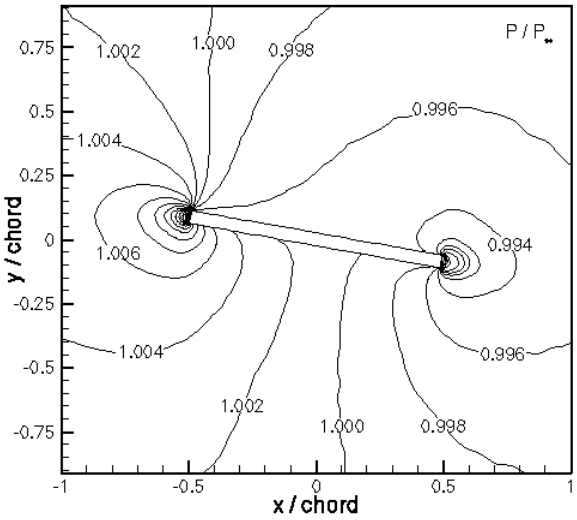

Fig. 6. Pressure ratio contours at 10 deg. angle of attack.

The computed aerodynamic characteristics of the 5% flat plate at Re=4 are shown in Figs. 7. The continuum results in Figs. 7 are obtained through solution of the Navier-Stokes equations including the usual first-order velocity slip boundary condition at the wall. The magnitude of difference between the CFD and IP results is sufficiently large that experimental measurements should be able to indicate which method is more physically accurate. The ratio of lift to drag is less than 1 at Re=4, which agrees with Miyagi's result.[22] From the IP results, the lift slope is about 3.82, which is smaller than 5.8 when Re=4,000. The same trend exists for NACA0009 airfoil at higher Reynolds numbers (Sunada et al.,[21]) with 2.9 at Re=4,000 and 5.5 at 40,000. Ultimately, we hope to verify the IP method using new experimental data (see Section 3).

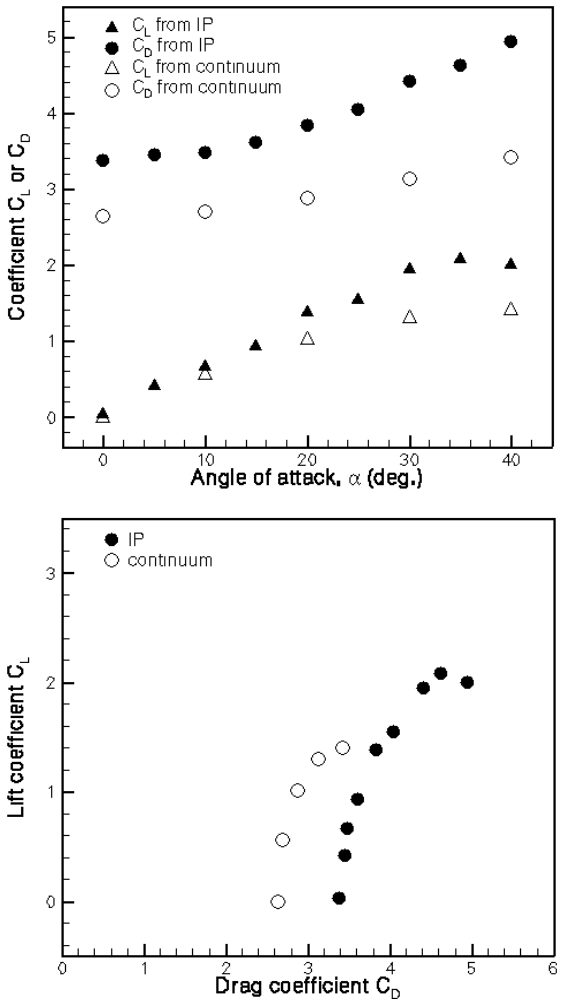

Fig. 7. Computations of the aerodynamic characteristics of a 5% flat plate at Re=4.

2.3 Hybrid Particle-Continuum Method

As micro scale gas flows are usually subsonic, modeling these flows involves a domain that is much larger than the system itself, which means that most of the domain can be described by the continuum equations. Since continuum solvers are several orders of magnitude more effective than the direct simulation Monte Carlo (DSMC) method,[6] an effective approach for micro scale gas flows is to combine the accuracy of kinetic methods and the efficiency of continuum solvers. Namely, hybrid techniques reduce the computational cost of a numerical simulation by limiting particle methods to the regions where the kinetic equations must be applied, and use continuum methods in the majority of the computational domain.

Compared with particle methods, computational fluid dynamics is well developed. In our hybrid approach (described in more detail in Ref. 12), the continuum approach solves the compressible Navier-Stokes equations using a finite volume formation. The fluxes are evaluated with a second-order accurate modified Steger-Warning flux-vector splitting approach.[23] In order to extend the validity of the Navier-Stokes equations, slip wall boundary conditions are implemented with the use of the Maxwell-type slip velocity expression. Characteristic boundary conditions[24] are used for open boundaries. In our adaptive hybrid approach, the IP method acts as the kinetic method while the Navier Stokes solver is used in the continuum domain. Both solvers are implemented in the MONACO system, which was first developed by Dietrich and Boyd[25] as a DSMC code. The continuum domain and the IP domain are separated by an interface. Through the interface, the continuum domain and the IP domain exchange information in every time step. The interface is time adaptive, and its location is determined by a continuum breakdown parameter.

Buffer cells and reservoir cells are used in the continuum domain as illustrated in Fig. 8. These buffer cells and reservoir cells are also treated as particle cells for particle movement and particle collisions. Then the interface becomes the internal cell edge for the IP treatment. The reservoir cells are used to generate particles that can enter the IP domain, which avoids directly generating particles on the interface. The buffer cells, however, improve the quality of the particles that enter the IP domain. Here is the algorithm for this strategy.

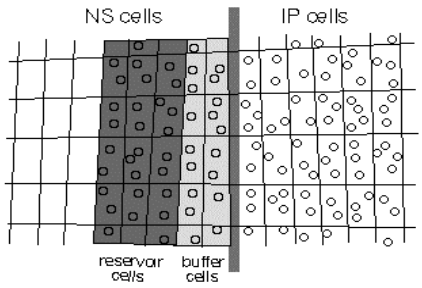

Fig. 8. Schematic of the interface between continuum (NS) and kinetic (IP) regions in the hybrid method.

1) Particles are generated in the buffer cells according to the Chapman-Enskog distribution based on the local macroscopic information.

2) During each time step, particles are generated in the reservoir cells according to the Chapman-Enskog distribution.

3) Particles in the buffer cells and reservoir cells are selected for collisions and move around using general IP procedures. The particles leaving particle cells (including buffer cells and reservoir cells) are removed.

4) Particles remaining in the reservoir cells are removed.

5) Steps 2-4 are repeated until the simulation is finished.

Obviously, more buffer cells used for the interface will improve the interface properties. However, this will increase the computational task, which contradicts the intention of hybrid schemes. Hence, only a few levels of buffer cells are used. The number of reservoir cells is also determined such that a negligible number of particles will enter any buffer cell from a continuum cell during one time step. Generally, two or more levels of reservoir cells are required.

Hybrid schemes can couple two methods by an interface because both methods are valid around the interface. In order to achieve the maximum benefit from a hybrid scheme, the interface should be placed in locations where continuum equations tend to breakdown. Hence, a continuum breakdown parameter should be adopted to determine the interface location. The Navier-Stokes equations can be derived from the Boltzmann equation using the Chapman-Enskog theory under near equilibrium conditions.[18] This analysis indicates that the Navier-Stokes equations are not valid when the nonlinear terms in the Chapman-Enskog expansion become important. In other words, the continuum equations break down when the velocity distribution function deviates from its equilibrium state by some degree. In fact, all the breakdown parameters in the literature are a combination of the coefficients in the first order Chapman-Enskog expansion. We employ the continuum breakdown parameter proposed by Garcia et al.[26] $B = \max\left\{\left|\tau^*_{i,j}\right|, \left|q^*_{i,j}\right|\right\}$ where $\tau^*_{i,j}$ is a normalized shear stress tensor, and $q^*_{i,j}$ is a normalized heat flux tensor. We use this parameter because it includes all the coefficients in the first-order Chapman-Enskog expansion. Numerical experiments are performed to determine an effective cutoff value for the breakdown parameter B.

For subsonic external micro-scale gas flows, a hybrid approach is a good choice for simulation because most of the computational domain can be described by the continuum equations. An air flow with a free stream Mach number of 0.2 over a 20-micron-long flat plate is simulated here. The free stream temperature and the wall temperature are 295K, and the body-length global Knudsen number of the flow is about 0.024 (the Reynolds number is about 2.4). Full thermal accommodation is assumed in the simulation. A computation domain is set up with 60 microns in the upstream region, 130 microns in the downstream region and a full span of 120 microns. Characteristic boundary conditions are adopted. About 20 particles are used for every particle cell, and the time step is less than the mean collision time of the molecules.

Figure 9 shows the velocity profiles from the full IP method, the hybrid approach, and the Navier-Stokes solver. For the hybrid result in Fig. 9, the cutoff value of the parameter B is 0.005, and the dashed line indicates the interface. The overall agreement of the results from three methods is good. This is not surprising because the flow is in the slip regime. A more detailed comparison is presented in Fig. 10 in terms of pressure coefficient, skin friction coefficient, and slip velocity. The cutoff value of B is 0.002 for hybrid 1, 0.005 for hybrid 2, and 0.01 for hybrid 3. As can be seen, the surface pressure is very similar for all cases except the result from hybrid 3. It is found that the shear stress on the surface and the slip velocity decrease when the IP domain shrinks. The continuum solver predicts the surface pressure well, while it only gives fair shear stress and under predicts the slip velocity. It seems 0.002 is an acceptable value of the continuum breakdown parameter B for this flow.

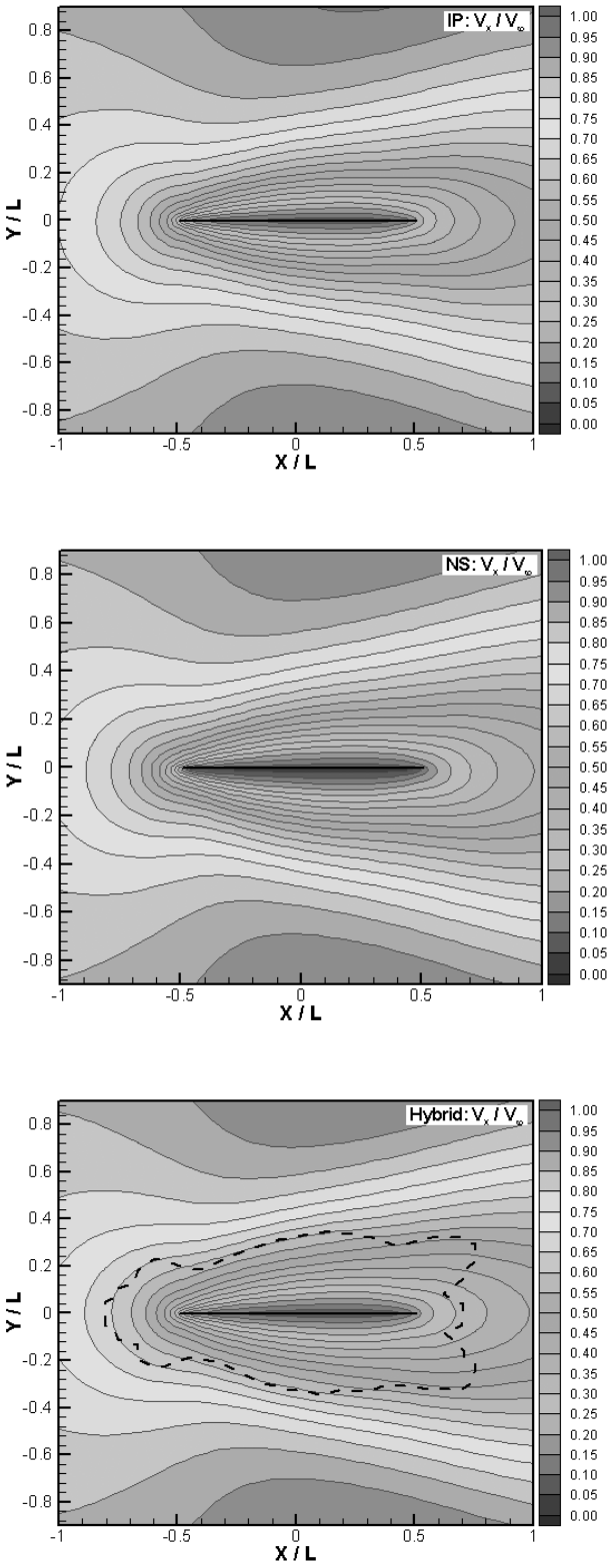

Fig. 9. Velocity contours around a flat plate computed with NS, IP, and hybrid methods.

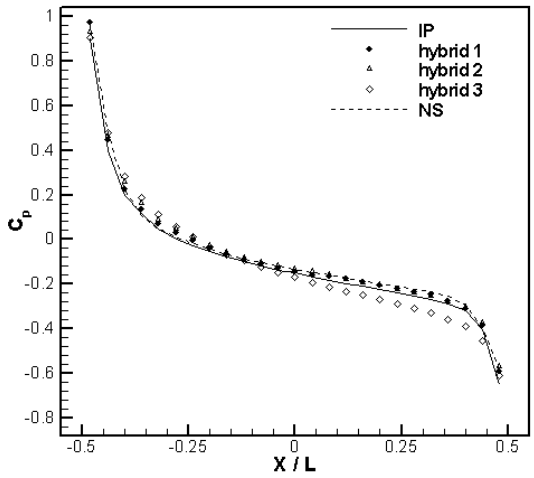

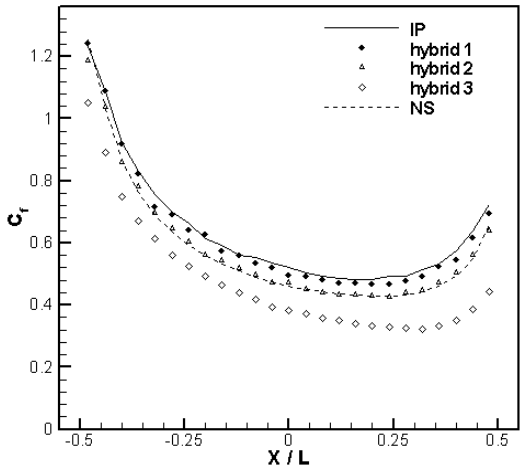

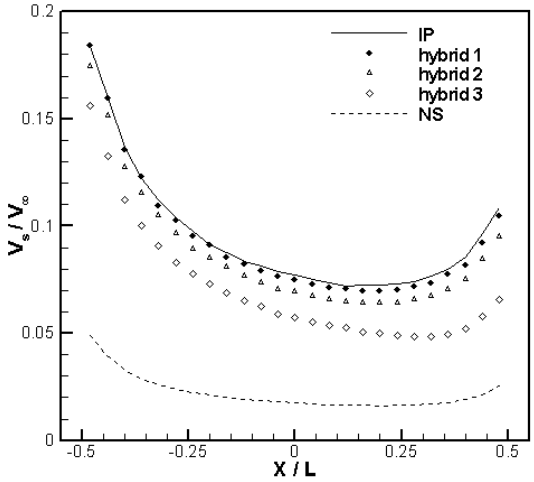

Fig. 10. Surface properties on a flat plate computed with NS, IP, and hybrid methods.

3. Experimental Studies

Due to the almost complete lack of suitable experimental data on micro-scale aerodynamics for assessment of the IP and hybrid flow codes, we have undertaken the generation of such data ourselves. The approach adopted is to test micro-fabricated airfoils in a low-turbulence wind-tunnel. Detailed discussions of these activities are provided in Refs. 27 and 28, respectively.

3.1 Sensor Design

Structural considerations limit the maximum chord of any micro-scale airfoil, and the width of the facility. For initial design, a 1 cm long, 1.5 μm thick crystalline silicon airfoil is being fabricated, with chords ranging from 20 to 100 μm. This size then leads to an expected force range from 0.05 mN to 0.6 mN. Previous researchers have measured forces on a beam system using piezoresistive methods, usually to measure a one-dimensional force.[29] Previous attempts to create a structure for measuring in 2 dimensions have entailed creation of a three-dimensional structure,[30] or measurement of two resistance components within the same structure.[31] The device used for these measurements allows simultaneous measurement of lift and drag, by using an asymmetric mounting. Sensor sensitivity was determined by using the ANSYS commercial finite element code, and 50 μm by 10 μm sensor regions were used.

The device is fabricated from a silicon-on-insulator wafer. The completed structure consists of the airfoil, and four resistor regions, which transmit the forces to the substrate. These resistors are then tied into four separate Wheatstone Bridges to allow easy measurement of their resistance changes. The design, which integrates the force sensor with the flat plate airfoil, is shown in Fig. 11. Figure 12 shows a photograph of an actual 20 micron chord-length airfoil and sensor structure, before under-etching of the airfoils.

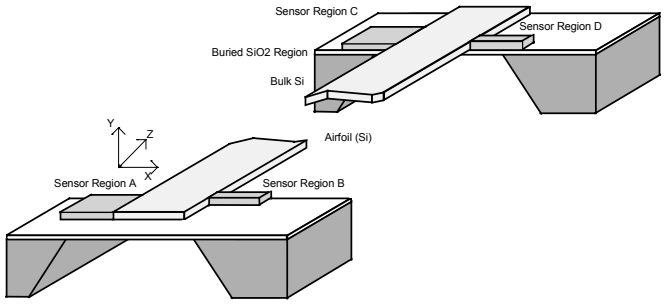

Fig. 11. Schematic of the integrated flat plate airfoil and sensor design.

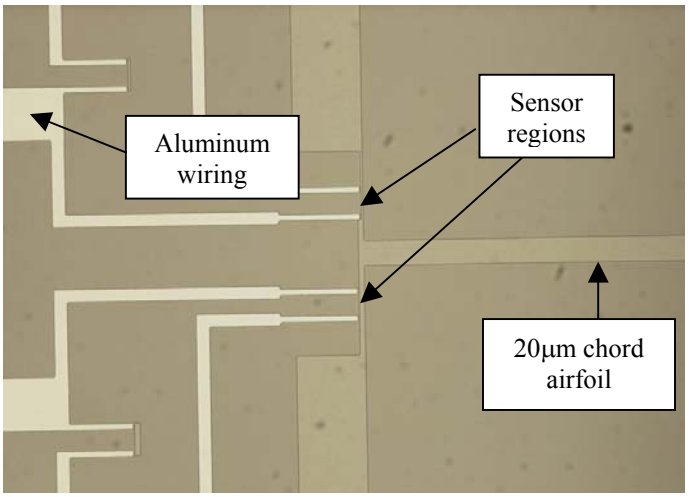

Fig. 12. Photograph of a micro-fabricated airfoil.

3.2 Facility Design

Because of the relative lack of flow visualization technology at the MEMS scale, this experiment is designed to measure lift and drag force on micromachined airfoils. A modified Blasius boundary layer solution, using a slip boundary condition, shows that on airfoils with a chord of less than 100 μm, the slip flow effects will cause a reduction in drag of 1-10 %, depending on conditions.[32] Computational results for flow over a 20 μm flat plate, performed using a hybrid particle-continuum method, show larger forces than the Blasius solution, but the same relative decrease in drag due to slip effects.[11]

Our sensor analysis[29] has shown that an integrated micro-device, as shown in Fig. 11, incorporating a flat-plate airfoil with piezoresistive sensors, can measure lift and drag on airfoils with chords ranging from 10 to 100 μm. In order to maximize rarefied flow effects, the airfoils are designed with a thickness of approximately 1 μm. Based on the expected forces on the airfoils, structural considerations limit the maximum span of the devices to approximately 1 cm. Because the piezoresistive sensors are integrated to the side of the airfoil, the maximum width of the test section for these airfoils is also 1cm. The facility is designed to allow pressure to be varied from 0.1 to 1.0 atmospheres, with a velocity range of 30 to 100 m/s. This approach allows independent control of Knudsen number and Reynolds number for a given test airfoil. Turbulence intensity should be kept as close to zero as possible for these experiments, to allow easier comparison of results, and to avoid velocity fluctuations within the system that may be of the same order of magnitude as the slip velocities at the surface of the airfoil. A schematic of the facility is shown in Fig. 13.

The small size of the test section allows for conventional methods of turbulence control to be carried to their limits. Both theoretical and experimental studies[33,34] have shown that stream-wise turbulence is reduced by contractions in the flow.

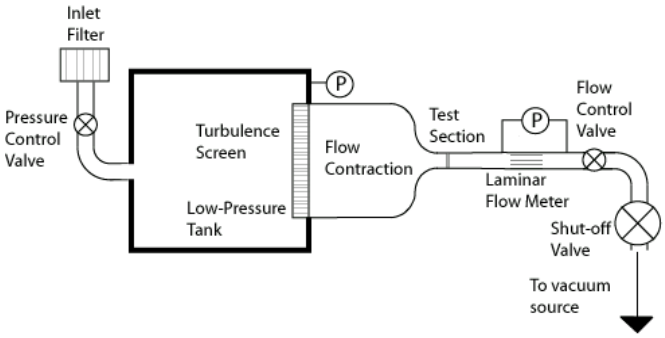

Fig. 13. Schematic of the test facility.

Typical wind-tunnel facilities use a 25:1 or 16:1 ratio contraction for turbulence suppression. Because of the small size of the micro-scale facility, a 100:1 ratio inlet can be used. A major difficulty in design of this facility involves the shape of the contraction section. While there has been much work on the design of both axisymmetric and square wind-tunnel contractions[35], the high contraction ratio, and small size, of this contraction are unique. A commercial CFD solver[36] was used to study several 100:1 square inlet configurations, with a final width of 1 cm. All potential configurations were studied with final velocities of 30 and 100 m/s, at a pressure of 1 atmosphere. Following the same approach as previous researchers, the contraction was built from two curves, meeting at an inflection point. To simplify the analysis, the curves chosen were circles, and the inflection point was taken as the midpoint of the converging section.

A laminar flow solver was used to compute the flow on a 20 by 20 by 60 mesh. The velocity profile at the end of the contraction, as well as 1 cm into the test section, were compared based on boundary layer thickness and free-stream velocity thickness. The best solutions were then re-tested at final velocities of 30 and 100 m/s, and pressures of 0.1 and 1.0 atmospheres. The results show that the shortest inlet possible is the most effective design for this application. The facility was subsequently fabricated, and is shown in Fig. 14. The flow direction of the tunnel in this photograph is from right to left.

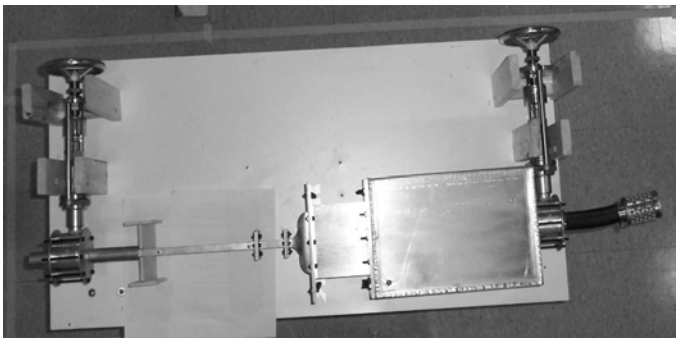

Fig. 14. Photograph of the micro-scale wind tunnel facility.

The air is drawn in through a small-engine air filter, and passes through a gated flow-control valve. The air is then drawn through a 30 cm long settling chamber, which has a 20 cm by 20 cm cross-section. Even at peak flow, the velocities in the settling chamber will remain below 1 m/s. At the end of the settling chamber, the air is drawn through a honeycomb of 0.2 cm diameter straws, as shown in Fig. 15. The air then travels down a 10 cm straight section, and into the 100-1 contraction, which is shown in Fig. 16. Immediately after the contraction is the test section. After the test section, the air flows through a laminar flow meter, and through a second gated flow control valve. This valve is used to regulate the operation pressure of the system. The system is then connected to a vacuum line.

The velocity in the test section was measured 1 cm into the test section at a pressure of 1.0 atmospheres, using a TSI Model 1279 hot wire probe. Figure 17 shows the turbulence intensity, normalized using the local average velocity. All results for local turbulence intensities are below 1%.

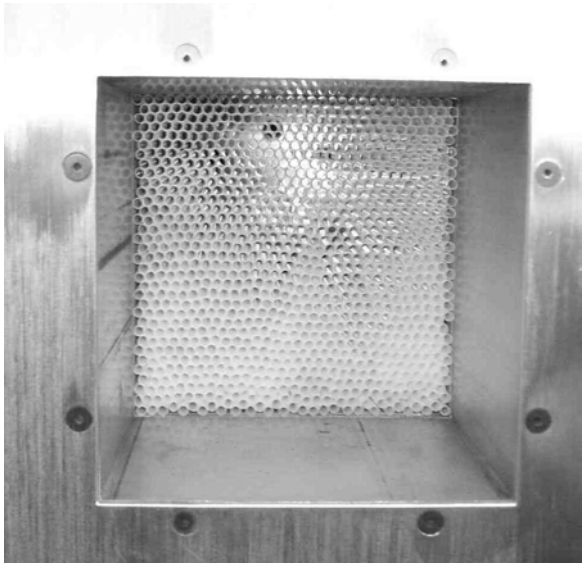

Fig. 15. Photograph of the turbulence screen.

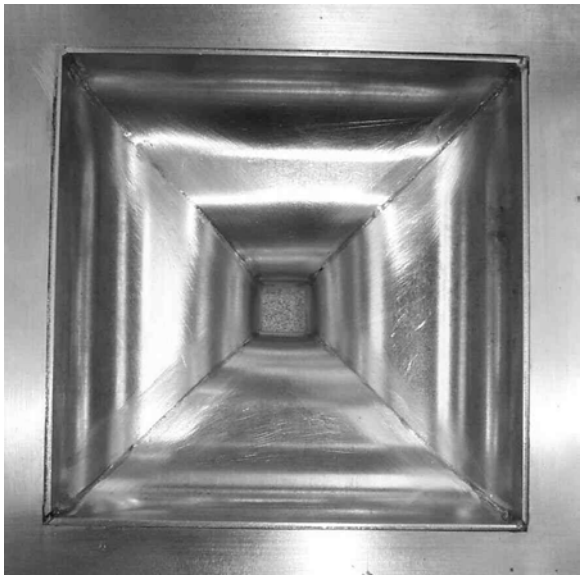

Fig. 16. Photograph of the contraction section.

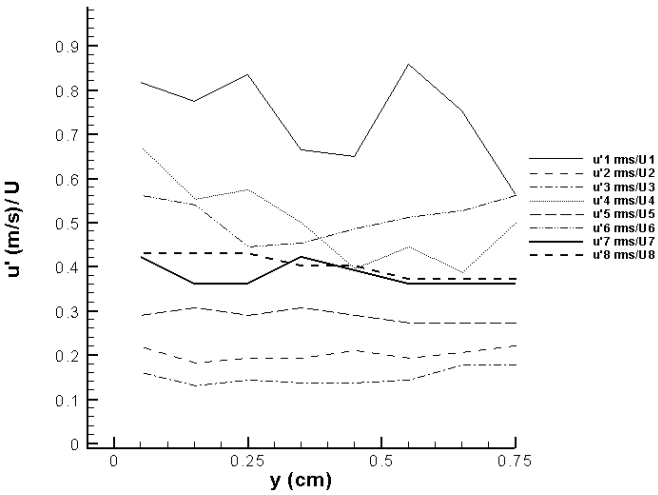

Fig. 17. Normalized turbulent fluctuations at 1 cm into the test section measured with a hot wire.

4. Conclusions

The study of micro-scale aerodynamics presents challenges to both numerical and experimental investigation. In our work, we have developed a number of numerical methods for studying these flow conditions. Much of our work centers on the Information Preservation (IP) method. A key success of this method is its ability to significantly reduce statistical fluctuations associated with the more mature DSMC method when applied to low-speed micro-scale gas flows. The IP method was compared with available experimental data and other numerical methods for a variety of micro-scale flows including channels, flat plates, and airfoils. For subsonic micro-scale flow over inclined flat plates, it was realized that much of the flow away from the plate was in the continuum regime. This motivated the development of a hybrid continuum-particle method where the IP technique provides the interface between the continuum and particle regimes.

Due to an almost complete lack of micro-scale aerodynamics measurements, we undertook the design and implementation of an experiment to test micro-fabricated airfoils with integrated sensors in a low-turbulence wind-tunnel. Measured data is expected in the next few months and will provide an ultimate test of the new numerical methods.

ACKNOWLEDGMENTS

This work was supported by the Air Force Office of Scientific Research through MURI grant F49620-98-1-0433. The authors gratefully acknowledge the contributions to this work by Graham Candler, Luis Bernal, Katsuo Kurabayashi, and Jing Fan.

References

[1]Pong, K.C., Ho, C.M., Liu, J., and Tai, Y.C., "Non-linear Pressure Distribution in Uniform Microchannels," in ASME FED, Vol. 197, *Application of Microfabrication to Fluid Mechanics*, 1994, pp. 51-56

[2]Arkilic, E., Schmidt, M.A., and Breuer, K.S., "Gaseous Flow in Long Microchannels," *Journal of Micro Electro Mechanical Systems*, Vol. 6, 1997, pp. 2-7

[3]Oh, C.K., Oran E.S., and Cybyk, B.Z., "Microchannel Flow Computed with the DSMC-MLG," AIAA paper 95-2090, San Diego, California, June 1995

[4]Mavriplis, C., Ahn, J.C., and Goulard, R., "Heat Transfer and Flowfields in Short Microchannels Using Direct Simulation Monte Carlo," *Journal of Thermophysics and Heat Transfer*, Vol. 11 (4), 1997, pp. 489-496

[5]Cai, C., Boyd, I.D., Fan, J. and Candler, G.V., "Direct Simulation Method for Low-speed Microchannel Flows," AIAA *Journal of Thermophysics and Heat Transfer*, Vol. 14 (3), 2000, pp. 368-378

[6]Bird, G.A.*„ Molecular Gas Dynamics and the Direct Simulation of Gas Flows*, Oxford Science Publications, New York, 1994.

[7]Beskok, A., "Physical Challenges and Simulation of Micro Fluidic Transport," AIAA Paper 2001-0718, Reno, Nevada, January 2001

[8]Fan, J., and Shen, C., "Statistical Simulation of Low-Speed Rarefied Gas Flows," *Journal of Computational Physics*, Vol. 167, 2001, pp. 393-412.

[9]Fan, J., Boyd, I.D., Cai, C.P., Hennighausen, K. and Candler, G.V., "Computation of Rarefied Gas Flows Around a NACA 0012 Airfoil," *AIAA Journal*, Vol. 39 (4), 2001, pp. 618-625.

[10]Sun, Q. and Boyd, I.D., "A Direct Simulation Method for Subsonic, Microscale Gas Flows," *Journal of Computational Physics*, Vol. 179, 2002, pp. 400-425.

[11]Sun, Q., Boyd, I.D., and Candler, G.V., "Numerical Simulation of Gas Flow Over Micro-Scale Airfoils," *Journal of Thermophysics and Heat Transfer*, Vol. 16, 2002, pp. 171-179.

[12]Sun, Q., Boyd, I.D., and Candler, G.V., "A Hybrid Continuum/Particle Approach for Micro-Scale Gas Flows," 23rd International Symposium on Rarefied Gas Dynamics, Whistler, Canada, July 2002.

[13]Fan, J., and Shen, C., "Statistical Simulation of Low-Speed Unidirectional Flows in Transition Regime," in *Rarefied Gas Dynamics*, edited by R. Brun, et al., (Cepadus-Editions, Toulouse, 1999), Vol. 2, 1999, pp. 245-252

[14]Schaaf, S.A. and Sherman, F.S., "Skin Friction in Slip Flow," *Journal of the Aeronautical Sciences*, Vol. 21 (2), 1954, pp. 85-90

[15]Mirels, H., "Estimate of Slip Effect on Compressible Laminar-Boundary-Layer Skin Friction," NACA TN 2609, 1951.

[16]Dennis, S.C. and Dunwoody, J., "The Steady Flow of a Viscous Fluid past a Flat Plate," *Journal of Fluid Mechanics*, Vol. 24 (3), 1966, pp. 577-595

[17]Tamada, K. and Miura, H., "Slip Flow Past a Tangential Flat Plate at Low Reynolds Numbers," *Journal of Fluid Mechanics*, Vol. 85 (4), 1978, pp. 731-7427

[18]Gombosi, T.I., *Gaskinetic Theory*, Cambridge University Press, Cambridge, 1994.

[19]Janour, Z., "Resistance of a Plate in Parallel Flow at Low Reynolds Numbers," *NACA* TM 1316, 1951.

[20]Churchill, S.W., *Viscous Flows: The Practical Use of the Theory*, Butterworth Publishers, Stoneham, 1988.

[21]Sunada, S. Sakaguchi, A. and Jawachi, K., "Airfoil Section Characteristics at a Low Reynolds Number," *Journal of Fluids Engineering*, Vol. 119, 1997, pp. 129-135

[22]Miyagi, T., "Oseen Flow Past a Flat Plate Inclined to the Uniform Stream," *Journal of the Physical Society of Japan*, Vol. 19(6), 1964, pp 1063-1073.

[23]MacCormack, R.W. and Candler, G.V., "The Solution of the Navier-Stokes Equations Using Gauss-Seidel Line Relaxation," *Computers and Fluids*, Vol. 17, 1989, pp. 135-150.

[24]Hirsch, C., *Numerical Computation of Internal and External Flows*, 1990.

[25]Dietrich, S., and Boyd, I.D., "Scalar and Parallel Optimized Implementation of the Direct Simulation Monte Carlo Method", *Journal of Computational Physics*, Vol. 126, 1996, pp. 328-342

[26]Garcia, A.L., Bell, J.B., Crutchfield, W.Y., and Alder, B.J., "Adaptive Mesh and Algorithm Refinement Using Direct Simulation Monte Carlo," *Journal of Computational Physics*, Vol. 154, 1999, pp. 134-155.

[27]Martin, M.J., Kurabayashi, K. and Boyd, I.D., "Measurement of Lift and Drag on MEMS Scale Airfoils in Slip Flow," *Proceedings of 2001 ASME Fluids Engineering Division Summer Meeting*, New Orleans, Louisiana, May 2001, Society of Mechanical Engineers, New York, NY.

[28]Martin, M.J., Boyd, I.D., and Bernal, L.P., "Design of a Low-Turbulence Facility for Micro-Scale Aerodynamics," *Proceedings of ASME FEDSM*, Paper FEDSM2002-31156, Montreal, Canada, July 2002.

[29]Sze, S. M., *Semiconductor Sensors*, John Wiley and Sons, New York, 1994.

[30]Chui, B.W., Kenny, T.W., Mamin, H.J., Terris, B.D. and Rugar, D., "Independent Detection of Vertical and Lateral Forces with a Sidewall-Implanted Dual-Axis Piezoresistive Cantilever", *Proceedings of IEEE MicroElectroMechanical Systems Workshop*, 1998, p.12.

[21]Brugger, J., Buser, R.A. and de Rooji, N.F., "Silicon cantilevers and tips for scanning probe microscopy," *Sensors and Actuators A*, Vol. 34, 1992, pp. 193-199.

[32]Martin, M.J. and Boyd, I.D., "Blasius Boundary Layer Solution With Slip Flow Conditions," *Proceedings of the 22nd International Symposium on Rarefied Gas Dynamics*, AIP, Melville, 2001, p. 518.

[33]Batchelor, G. K.*, Theory of Homogeneous Turbulence*, Cambridge University Press, Cambridge, UK, Chap. 4., 1953.

[34]Uberoi, M. S., "Effect of Wind-Tunnel Contraction on Free Stream Turbulence," *Journal of the Aeronautical Sciences*, Vol. 23(8), 1956, pp. 754-764.

[35]Mikhail, M. N., and Rainbird, W. J., "Optimum Design of Wind Tunnel Contractions," AIAA Paper 1978-819, 1978.

[36]FLUENT/UNS user's guide: release 3.2. 1995, Fluent Inc. Lebanon, NH.